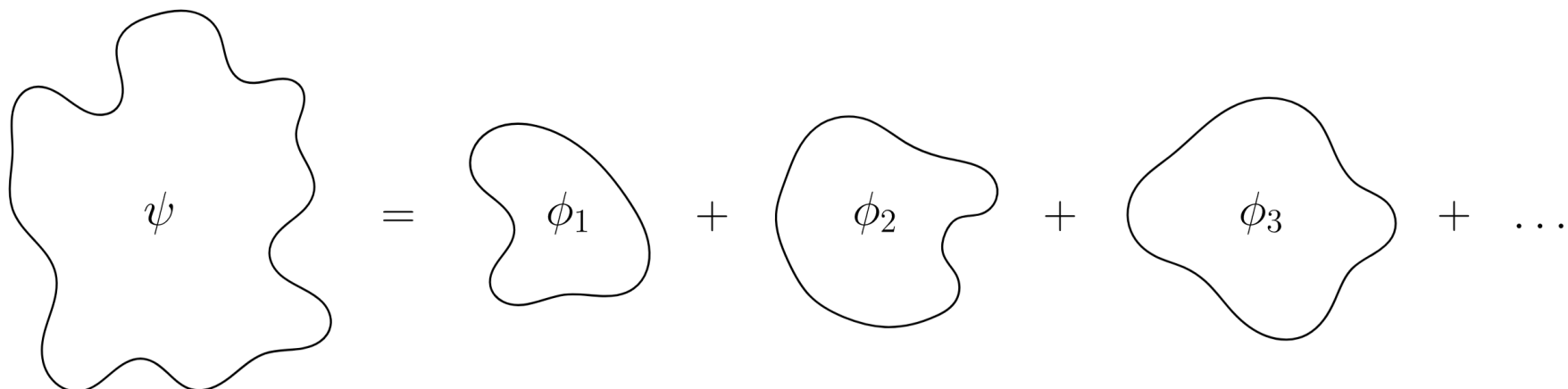


Graphical Stabilizer Decompositions for Multi-Control Toffoli Gate Dense Quantum Circuits

Maturitätsarbeit

Yves Vollmeier

$$\psi = \phi_1 + \phi_2 + \phi_3 + \dots$$


Supervised by Dr. Riccardo Ferrario

Mathematisch Naturwissenschaftliches Gymnasium Rämibühl

January 31, 2025

Table of contents

1. Motivation

2. Graphical Languages ←

3. Stabilizer Decompositions ← *Graphical
Stabilizer Decompositions
for Multi-Control Toffoli Gate Dense Quantum Circuits*

4. Applications ←

5. Summary

1. Motivation

Looking at cutting-edge research

arXiv > quant-ph

Quantum Physics

Authors and titles for January 2025

Total of 903 entries : 1-50 51-100 101-150 151-200 ... 901-903
Showing up to 50 entries per page: [fewer](#) | [more](#) | [all](#)

[1] arXiv:2501.00010 [pdf, other]

Coordinate Space Modification of Fock's Theory-Harmonic Tensors in the Quantum Coulomb Problem

Sergei P. Efimov

Comments: 38 pages, 1 figure

Journal-ref: Phys. Usp.65(9):pp.952-967 (2022) (in russian)

Subjects: Quantum Physics (quant-ph); Atomic Physics (physics.atom-ph)

[2] arXiv:2501.00135 [pdf, html, other]

GroverGPT: A Large Language Model with 8 Billion Parameters for Quantum Searching

Haoran Wang, Pingzhi Li, Min Chen, Jinglei Cheng, Junyu Liu, Tianlong Chen

Comments: 12 pages including appendices

Subjects: Quantum Physics (quant-ph); Artificial Intelligence (cs.AI); Machine Learning (cs.LG)

[3] arXiv:2501.00173 [pdf, other]

The Aldous--Lyons Conjecture II: Undecidability

Lewis Bowen, Michael Chapman, Thomas Vidick

Comments: 207 pages, 17 figures

Subjects: Quantum Physics (quant-ph); Combinatorics (math.CO); Group Theory (math.GR); Probability (math.PR)

[4] arXiv:2501.00180 [pdf, html, other]

A Coherence-Protection Scheme for Quantum Sensors Based on Ultra-Shallow Single Nitrogen-Vacancy Centers in Diamond

Anton Pershin, András Tárkányi, Vladimir Verkhovlyuk, Viktor Ivády, Adam Gall

Comments: 11 pages, 5 figures

Subjects: Quantum Physics (quant-ph)

[5] arXiv:2501.00188 [pdf, html, other]

Optimal asymptotic precision bounds for nonlinear quantum metrology under collective dephasing

Francisco Ribéri, Lorenza Viola

Comments: 23 pages, 3 figures, 1 table

Subjects: Quantum Physics (quant-ph)

[6] arXiv:2501.00209 [pdf, html, other]

Unraveling the switching dynamics in a quantum double-well potential

Qile Su, Rodrigo G. Cortiñas, Jayameenakshi Venkatraman, Shruti Puri

Subjects: Quantum Physics (quant-ph)

[7] arXiv:2501.00280 [pdf, html, other]

Optimizing Global Quantum Communication via Satellite Constellations

Yichen Gao, Guangjun Song, Ting Zhu

Subjects: Quantum Physics (quant-ph); Emerging Technologies (cs.ET)

[8] arXiv:2501.00293 [pdf, html, other]

Optimal Control in Nearly-Adiabatic Two-Level Quantum Systems via Time-Dependent Resonance

Takayuki Suzuki

Subjects: Quantum Physics (quant-ph)

[9] arXiv:2501.00327 [pdf, html, other]

Investigating Pure State Uniqueness in Tomography via Optimization

Jiahui Wu, Zheng An, Chao Zhang, Xuanran Zhu, Shilin Huang, Bei Zeng

Comments: 13 pages, 3 figures

Subjects: Quantum Physics (quant-ph)

[10] arXiv:2501.00331 [pdf, html, other]

Q3DE: A fault-tolerant quantum computer architecture for multi-bit burst errors by cosmic rays

Yasunari Suzuki, Takanori Sugiyama, Tomochika Arai, Wang Liao, Koji Inoue, Teruo Tanimoto

Comments: Published in 2022 55th IEEE/ACM International Symposium on Microarchitecture (MICRO)

Journal-ref: 2022 55th IEEE/ACM International Symposium on Microarchitecture (MICRO), Chicago, IL, USA, 2022, pp. 1110-1125

Subjects: Quantum Physics (quant-ph); Hardware Architecture (cs.AR)

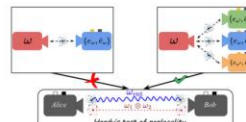
Quantum
the open journal for quantum science

PAPERS PERSPECTIVES

Doi, title, author, arXiv id, ...

Quantum has published 1613 Papers in 9 Volumes, as well as 84 Views in Quantum Views.

SEARCH

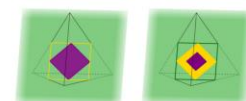


PAPER

Bipartite polygon models: entanglement classes and their nonlocal behaviour

Mayalakshmi Kolangatt, Thigazholi Muruganandan, Sahil Gopalkrishna Naik, Tamal Guha, Manik Banik, and Sutapa Saha, Quantum 9, 1599 (2025).

Hardy's argument constitutes an elegantly logical test for identifying nonlocal features of multipartite correlations. In this paper, we investigate Hardy's nonlocal behavior within a broad...

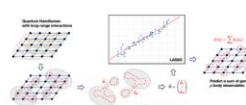


PAPER

Can QBism exist without Q? Morphophoric measurements in generalised probabilistic theories

Anna Szymusiak and Wojciech Slomczyński, Quantum 9, 1598 (2025).

In a Generalised Probabilistic Theory (GPT) equipped additionally with some extra geometric structure we define the morphophoric measurements as those for which the measurement map sending s...

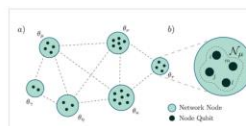


PAPER

Efficient Learning of Long-Range and Equivariant Quantum Systems

Štěpán Šmid and Roberto Bondesan, Quantum 9, 1597 (2025).

In this work, we consider a fundamental task in quantum many-body physics – finding and learning ground states of quantum Hamiltonians and their properties. Recent works have studied the tas...



PAPER

Private and Robust States for Distributed Quantum Sensing

Luis Bugallo, Majid Hassani, Yasser Omar, and Damian Markham, Quantum 9, 1596 (2025).

Distributed quantum sensing enables the estimation of multiple parameters encoded in spatially separated probes. While traditional quantum sensing is often focused on estimating a single par...

ZX-calculus

Dynamic T-decomposition for classical simulation of quantum circuits
Wira Azmoon Ahmad and Matthew Sutcliffe
[Show abstract](#) ↴ [Show bibdata](#) ↴

arXiv:2412.17182
Keywords: Classical Simulation, PyZX, Applied, Automation, Clifford+T.

Towards Faster Quantum Circuit Simulation Using Graph Decompositions, GNNs and Reinforcement Learning
Alex Koziell-Pipe, Richie Yeung and Matthew Sutcliffe
[Show abstract](#) ↴ [Show bibdata](#) ↴

38th Conference on Neural Information Processing Systems (NeurIPS 2024)
Keywords: Classical Simulation, Automation, PyZX, Applied, ZX-Calculus, Clifford+T.

Floquetifying stabiliser codes with distance-preserving rewrites
Benjamin Rodatz, Boldizsár Poór and Aleks Kissinger
[Show abstract](#) ↴ [Show bibdata](#) ↴

arXiv:2410.17240
Keywords: Error Correcting Codes, Clifford Fragment, Applied.

Dynamical weight reduction of Pauli measurements
Julio C. Magdalena de la Fuente
[Show abstract](#) ↴ [Show bibdata](#) ↴

arXiv:2410.12527
Keywords: MBQC, Phase gadgets, Optimisation, Applied.

Generalized flow for hypergraph measurement patterns
Martin van IJcken
[Show abstract](#) ↴ [Show bibdata](#) ↴

University of Oxford Masters Thesis
Keywords: MBQC, gflow, ZH-calculus, Master Thesis.

Categorical quantum theory and percolation methods for measurement-based quantum computing
Joe Bacchus George
[Show abstract](#) ↴ [Show bibdata](#) ↴

University of Oxford Masters Thesis
Keywords: MBQC, Pauli Fusion, Photons, ZX-calculus, Master Thesis.

Fusion and flow: formal protocols to reliably build photonic graph states
Giovanni de Felice, Boldizsár Poór, Lia Yeh and William Cashman
[Show abstract](#) ↴ [Show bibdata](#) ↴

arXiv:2409.13541
Keywords: Photons, Pauli Fusion, MBQC, gflow, Protocols.

Parallel Quantum Circuit Extraction from MBQC-Patterns
Marcel Quanz, Korbinian Staudacher and Karl Fürlinger
[Show abstract](#) ↴ [Show bibdata](#) ↴

2024 IEEE International Parallel and Distributed Processing Symposium Workshops (IPDPSW)
Keywords: MBQC, ZX-calculus, Circuit Extraction, Applied.

Smarter k-Partitioning of ZX-Diagrams for Improved Quantum Circuit Simulation
Matthew Sutcliffe
[Show abstract](#) ↴ [Show bibdata](#) ↴

arXiv:2409.00828
Keywords: Classical Simulation, Automation, PyZX, Applied, ZX-Calculus, Clifford+T.

Magic of the Heisenberg Picture
Neil Dowling, Pavel Kos and Xhek Turkeshi
[Show abstract](#) ↴ [Show bibdata](#) ↴

arXiv:2408.16047
Keywords: Entanglement, Condensed Matter, Classical Simulation, ZX-calculus, Applied.

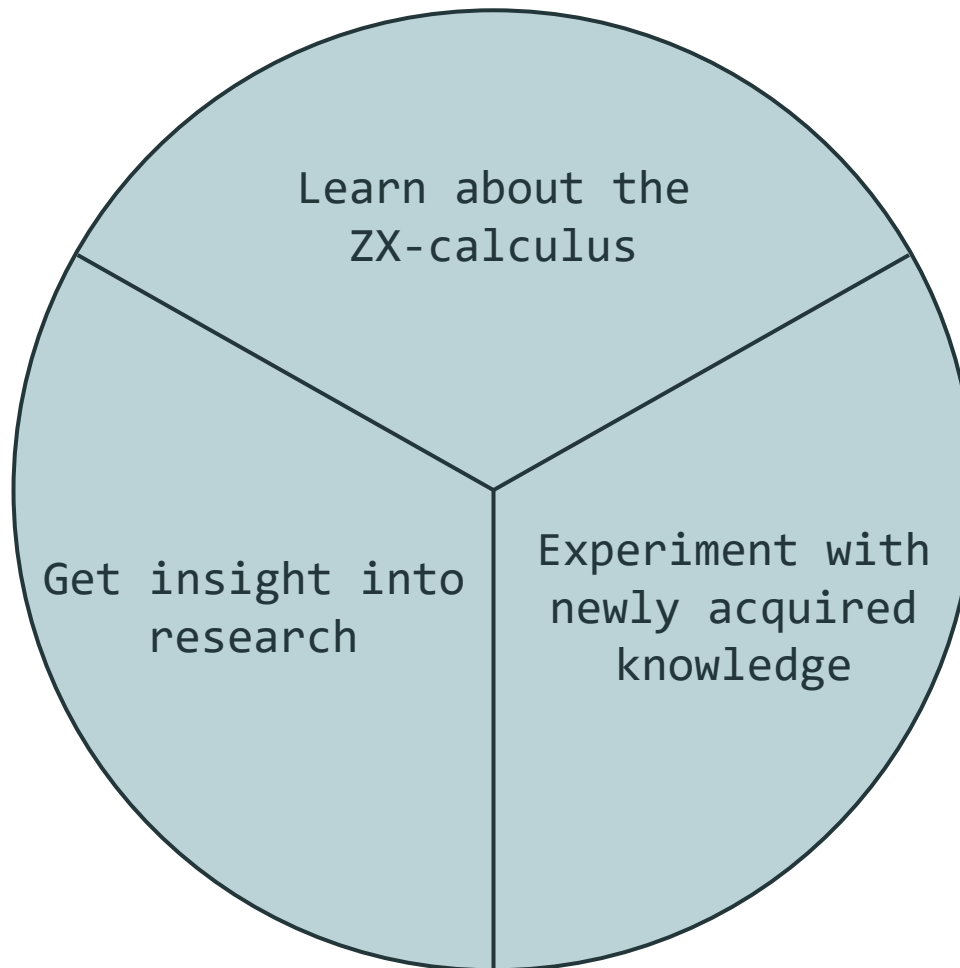
Redefining Lexicographical Ordering: Optimizing Pauli String Decompositions for Quantum Compiling
Qunsheng Huang, David Winderl, Arianne Meijer-van de Griend and Richie Yeung
[Show abstract](#) ↴ [Show bibdata](#) ↴

arXiv:2408.00354
Keywords: ZX-Supported, Optimisation, Automation.

Enhancing Encoding Rate through Alternate Floquetification
Yabo Wang, Yunlong Xiao, Kishor Bharti and Bo Qi
[Show abstract](#) ↴ [Show bibdata](#) ↴

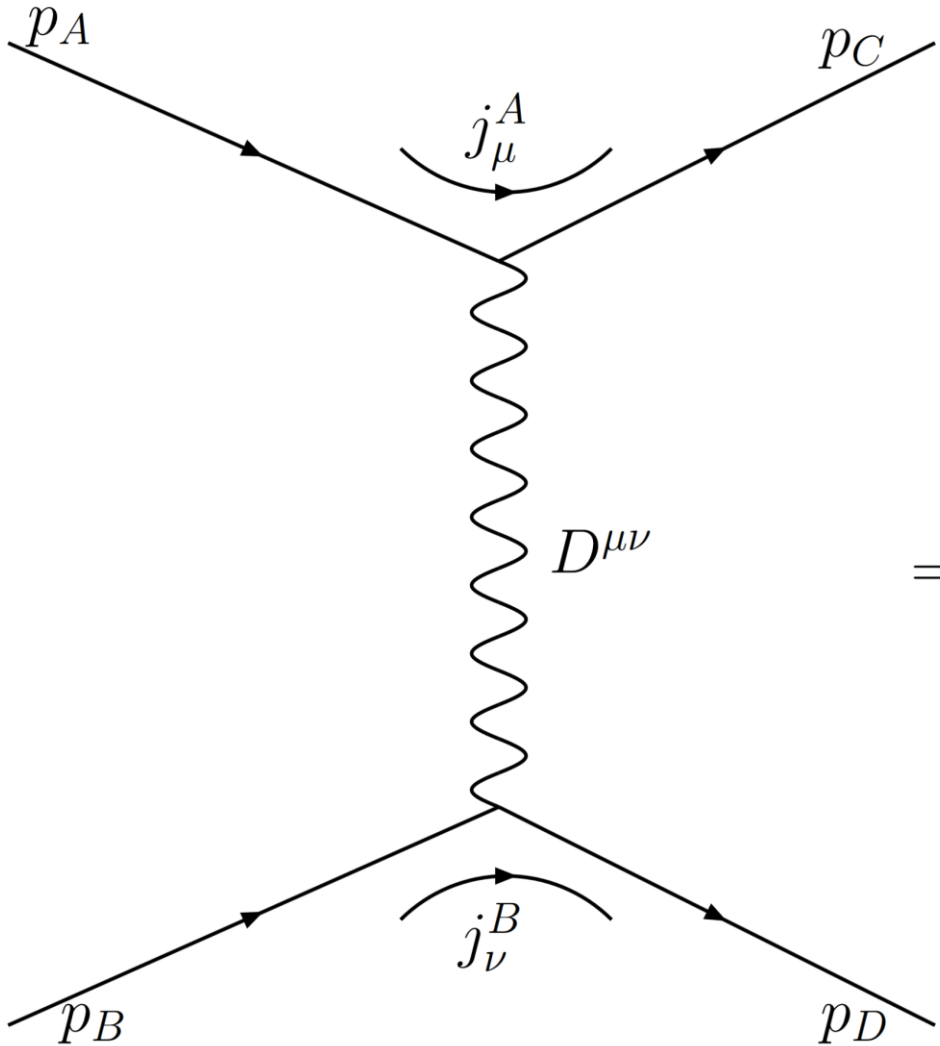
2024 43rd Chinese Control Conference (CCC)
Keywords: Error Correcting Codes, Applied, ZX-Calculus.

Goal of this Matura project



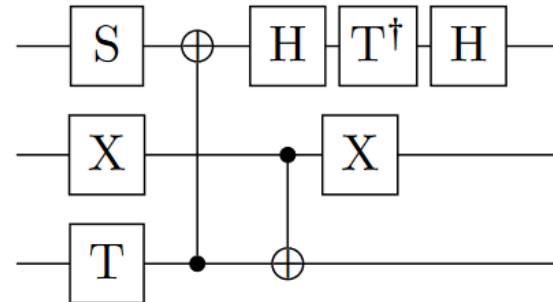
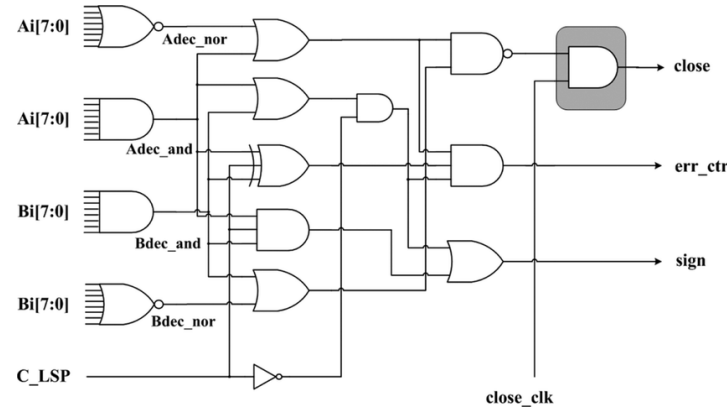
2. Graphical Languages

Feynman diagrams



$$= -i \int d^4x d^4y j_\mu^A(x) D^{\mu\nu}(x, y) j_\nu^B(y)$$

Other graphical languages



$$\begin{aligned}
 \text{Diagram 1: } & a \text{---} b \text{---} c = \theta_c^{ab}, \\
 \text{Diagram 2: } & a \text{---} b \text{---} c \text{---} d = \chi_{bcd}^a. \\
 \text{Diagram 3: } & a \text{---} f \text{---} c \text{---} d \text{---} e = (\theta_c^{af} + \gamma_c^{af}) \chi_{fde}^b
 \end{aligned}$$

Detailed description: Three hand-drawn Feynman-like diagrams are shown. Diagram 1 shows a loop with vertices a , b , and c , labeled $= \theta_c^{ab}$. Diagram 2 shows a chain of four vertices a , b , c , and d , labeled $= \chi_{bcd}^a$. Diagram 3 shows a more complex loop with vertices a , f , c , d , and e , labeled $= (\theta_c^{af} + \gamma_c^{af}) \chi_{fde}^b$.

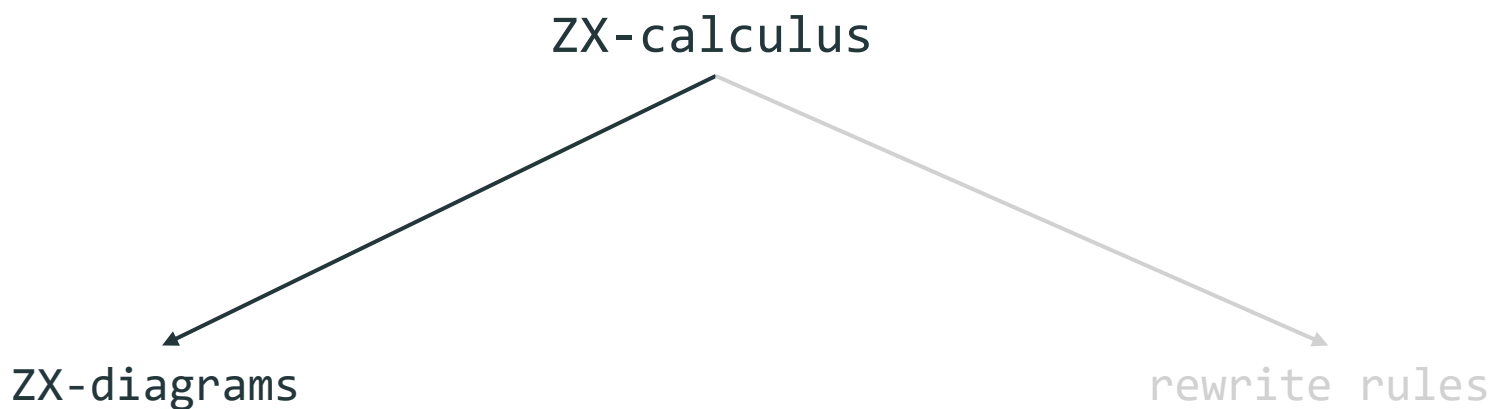
ZX-calculus

“The ZX-calculus is a rigorous graphical language for reasoning about linear maps between qubits, which are represented as string diagrams called ZX-diagrams.”

Definition 2.2.1 A *qubit* is an abstract representation of a single bit of information, represented as a state vector $|\psi\rangle$ in a two-dimensional Hilbert space

$$|\psi\rangle = \alpha|0\rangle + \beta|1\rangle, \quad \alpha, \beta \in \mathbb{C}, \quad (2.19)$$

where the vectors $|0\rangle := \begin{pmatrix} 1 \\ 0 \end{pmatrix}$ and $|1\rangle := \begin{pmatrix} 0 \\ 1 \end{pmatrix}$ form an orthonormal basis and are thus called *computational basis states*.



ZX-diagrams

ZX-diagrams are constructed by taking matrix products or tensor products⁴ of the following linear maps, so-called *generators*:

- *Z-spider:*

$$Z_m^n[\alpha] = m \left\{ \begin{array}{c} \text{:} \\ \text{:} \\ \text{:} \end{array} \begin{array}{c} \text{:} \\ \text{:} \\ \text{:} \end{array} \right\} n = |0\rangle^{\otimes n} \langle 0|^{\otimes m} + e^{i\alpha} |1\rangle^{\otimes n} \langle 1|^{\otimes m} \quad (3.3)$$

- *X-spider:*

$$X_m^n[\alpha] = m \left\{ \begin{array}{c} \text{:} \\ \text{:} \\ \text{:} \end{array} \begin{array}{c} \text{:} \\ \text{:} \\ \text{:} \end{array} \right\} n = |+\rangle^{\otimes n} \langle +|^{\otimes m} + e^{i\alpha} |- \rangle^{\otimes n} \langle -|^{\otimes m} \quad (3.4)$$

Remark 3.1.2 These generators form two families of linear maps that are given by

$$\{Z_m^n[\alpha] : (\mathbb{C}^2)^{\otimes m} \rightarrow (\mathbb{C}^2)^{\otimes n} \mid m, n \in \mathbb{N}, \alpha \in [0, 2\pi)\}$$

and

$$\{X_m^n[\alpha] : (\mathbb{C}^2)^{\otimes m} \rightarrow (\mathbb{C}^2)^{\otimes n} \mid m, n \in \mathbb{N}, \alpha \in [0, 2\pi)\}.$$

ZX-diagrams

- Vertical composition \Leftrightarrow Tensor product

$$\begin{array}{c} \text{---} \\ \text{---} \end{array} \circlearrowleft = \begin{pmatrix} 1 & 0 \\ 0 & 0 \\ 0 & 0 \\ 0 & 1 \end{pmatrix} \otimes \begin{pmatrix} 1 & 0 \\ 0 & 1 \end{pmatrix} = \begin{pmatrix} 1 & 0 & 0 & 0 \\ 0 & 1 & 0 & 0 \\ 0 & 0 & 0 & 0 \\ 0 & 0 & 0 & 0 \\ 0 & 0 & 0 & 0 \\ 0 & 0 & 0 & 0 \\ 0 & 0 & 0 & 0 \\ 0 & 0 & 1 & 0 \\ 0 & 0 & 0 & 1 \end{pmatrix}$$

$$\begin{array}{c} \text{---} \\ \text{---} \end{array} = \begin{pmatrix} 1 & 0 \\ 0 & 1 \end{pmatrix} \otimes \frac{1}{\sqrt{2}} \begin{pmatrix} 1 & 0 & 0 & 1 \\ 0 & 1 & 1 & 0 \\ 0 & 0 & 0 & 1 \\ 0 & 0 & 0 & 0 \end{pmatrix} = \frac{1}{\sqrt{2}} \begin{pmatrix} 1 & 0 & 0 & 1 & 0 & 0 & 0 & 0 \\ 0 & 1 & 1 & 0 & 0 & 0 & 0 & 0 \\ 0 & 0 & 0 & 1 & 0 & 0 & 0 & 1 \\ 0 & 0 & 0 & 0 & 0 & 1 & 1 & 0 \end{pmatrix}$$

- Horizontal composition \Leftrightarrow Matrix multiplication

$$\begin{array}{c} \text{---} \\ \text{---} \end{array} = \frac{1}{\sqrt{2}} \begin{pmatrix} 1 & 0 & 0 & 1 & 0 & 0 & 0 & 0 \\ 0 & 1 & 1 & 0 & 0 & 0 & 0 & 0 \\ 0 & 0 & 0 & 0 & 1 & 0 & 0 & 1 \\ 0 & 0 & 0 & 0 & 0 & 1 & 1 & 0 \end{pmatrix} \begin{pmatrix} 1 & 0 & 0 & 0 \\ 0 & 1 & 0 & 0 \\ 0 & 0 & 0 & 0 \\ 0 & 0 & 0 & 0 \\ 0 & 0 & 0 & 0 \\ 0 & 0 & 0 & 0 \\ 0 & 0 & 1 & 0 \\ 0 & 0 & 0 & 1 \end{pmatrix} = \frac{1}{\sqrt{2}} \begin{pmatrix} 1 & 0 & 0 & 0 \\ 0 & 1 & 0 & 0 \\ 0 & 0 & 0 & 1 \\ 0 & 0 & 1 & 0 \end{pmatrix}$$

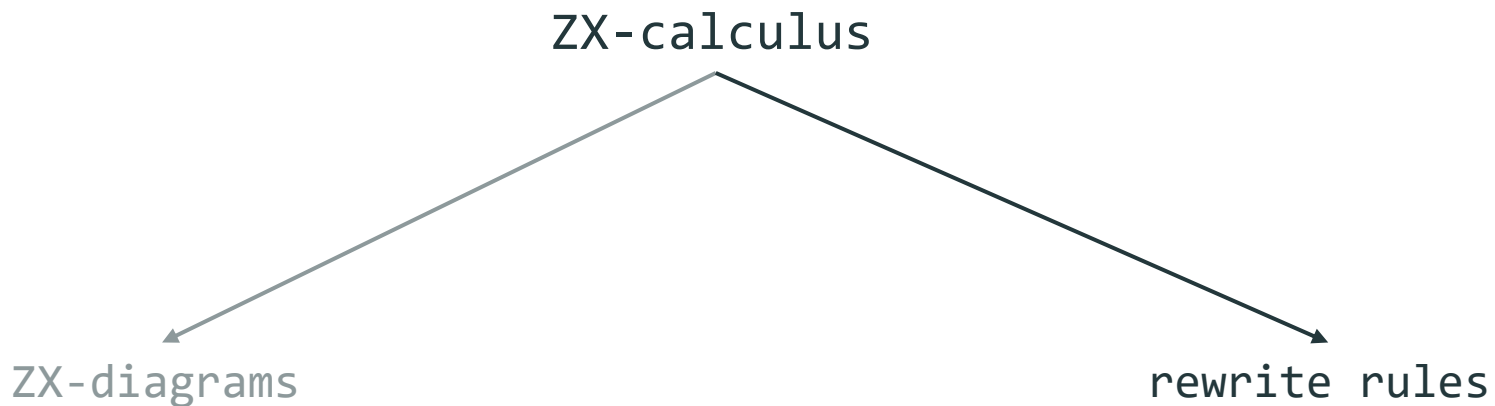
ZX-calculus

“The ZX-calculus is a rigorous graphical language for reasoning about linear maps between qubits, which are represented as string diagrams called ZX-diagrams.”

Definition 2.2.1 A *qubit* is an abstract representation of a single bit of information, represented as a state vector $|\psi\rangle$ in a two-dimensional Hilbert space

$$|\psi\rangle = \alpha|0\rangle + \beta|1\rangle, \quad \alpha, \beta \in \mathbb{C}, \quad (2.19)$$

where the vectors $|0\rangle := \begin{pmatrix} 1 \\ 0 \end{pmatrix}$ and $|1\rangle := \begin{pmatrix} 0 \\ 1 \end{pmatrix}$ form an orthonormal basis and are thus called *computational basis states*.



Rewrite rules

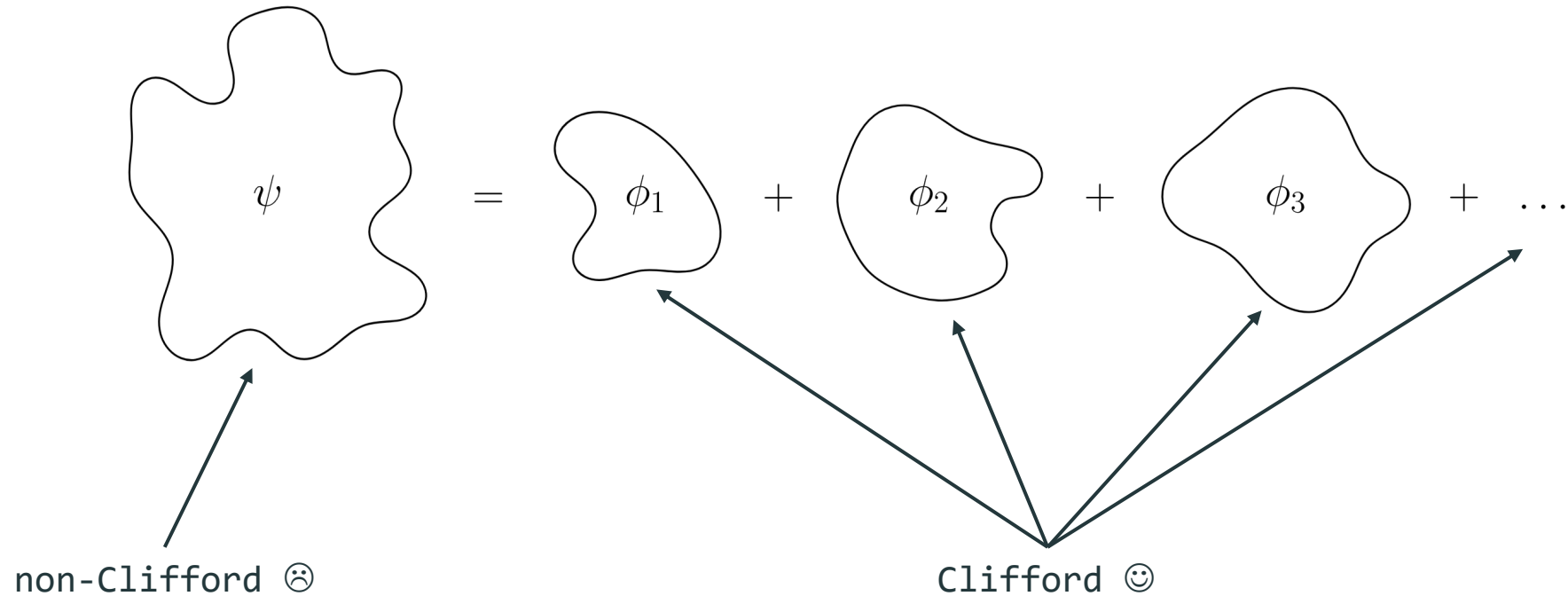
$$\begin{array}{c}
 \text{(sp)} = \text{---} \quad \text{(cc)} = \text{---} \\
 \text{---} \quad \text{---} \\
 \text{(π)} = \xi_1 \text{---} \quad \left. \begin{array}{c} \text{(c)} \\ \text{---} \end{array} \right\} n = \xi_2 \text{---} \\
 \text{---} \quad \left. \begin{array}{c} \text{---} \\ \text{---} \end{array} \right\} n \\
 m \left\{ \text{---} \right. \quad \text{(b)} = \xi_3 \quad m \left\{ \text{---} \right. \quad \text{(hh)} = \text{---} \\
 \text{---} \quad \left. \begin{array}{c} \text{---} \\ \text{---} \end{array} \right\} n \quad \text{---} \quad \text{---} \\
 \text{(ho)} = \xi_4 \quad \text{(id)} = \text{---} \quad \text{(eu)} = \xi_5 \text{---} \\
 \text{---} \quad \text{---} \quad \text{---} \quad \text{---} \\
 \xi_1 = e^{ia\alpha}, \xi_2 = \frac{e^{ia\alpha}}{\sqrt{2}^{n-1}}, \xi_3 = \sqrt{2}^{(n-1)(m-1)}, \xi_4 = \frac{1}{2}, \xi_5 = e^{-i\pi/4}
 \end{array} \tag{3.5}$$

(sp) spider fusion
(π) π -commutation rule
(b) bialgebra
(ho) hopf
(eu) euler decomposition of Hadamard

(cc) color change
(c) state copy
(hh) hadamard-hadamard cancellation
(id) identity

3. Stabilizer Decompositions

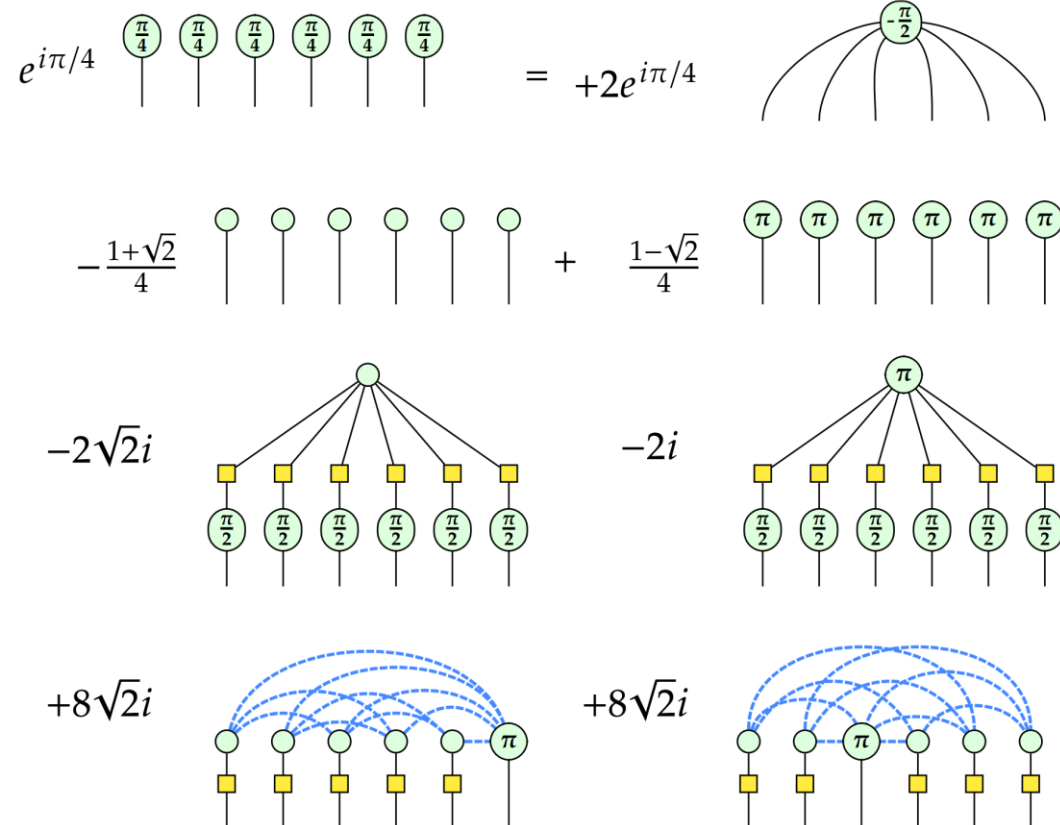
Stabilizer decompositions in a nutshell



⌚ or ☺ according to Gottesman-Knill theorem:

Theorem 2.3.1 Any quantum computer performing only: a) Clifford group gates, b) measurements of Pauli group operators, and c) Clifford group operations conditioned on classical bits, which may be the results of earlier measurements, can be perfectly simulated in polynomial time on a probabilistic classical computer.

Example: BSS decomposition



Scaling:

$$p^{t/r} = 2^{\alpha t} \implies \alpha = \frac{\log_2(p)}{r}$$

p number of terms

r number of non-Clifford terms reduced

$$\alpha = \log_2(7)/6 \approx 0.468$$

Considered class of diagrams

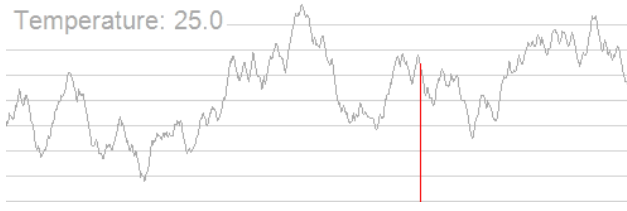
$$\text{---} \begin{array}{c} \nearrow \\ \searrow \end{array} = \begin{pmatrix} 1 & 1 \\ 0 & 1 \end{pmatrix}$$

$$\text{---} \begin{array}{c} \nearrow \\ \pi \end{array} = \text{---} \begin{array}{c} \pi \\ \nearrow \\ \searrow \end{array} = \begin{pmatrix} 1 & 0 \\ 1 & 1 \end{pmatrix}$$

$$\text{---} \begin{array}{c} \star \\ \nearrow \end{array} := \text{---} \begin{array}{c} \nearrow \\ \pi \end{array} = \text{---} \begin{array}{c} \pi \\ \nearrow \end{array} = \begin{pmatrix} 1 & 1 \\ 1 & 0 \end{pmatrix}$$

$$\text{---} \begin{array}{c} \star \\ \nearrow \end{array} \rightsquigarrow \text{---} \cdots$$

Novel decompositions



$$\begin{array}{c} \text{---} \\ \text{---} \\ \text{---} \\ \text{---} \\ \text{---} \end{array} = \xi_1 \begin{array}{c} \text{---} \\ \text{---} \\ \text{---} \\ \text{---} \\ \text{---} \end{array} + \xi_2 \begin{array}{c} \text{---} \\ \text{---} \\ \text{---} \\ \text{---} \\ \text{---} \end{array} + \xi_3 \begin{array}{c} \text{---} \\ \text{---} \\ \text{---} \\ \text{---} \\ \text{---} \end{array} \quad (4.23)$$

$$+ \xi_4 \begin{array}{c} \text{---} \\ \text{---} \\ \text{---} \\ \text{---} \\ \text{---} \end{array} + \xi_5 \begin{array}{c} \text{---} \\ \text{---} \\ \text{---} \\ \text{---} \\ \text{---} \end{array} + \xi_6 \begin{array}{c} \text{---} \\ \text{---} \\ \text{---} \\ \text{---} \\ \text{---} \end{array}$$

$$\xi_1 = -192, \xi_2 = \frac{15\sqrt{2}}{8}, \xi_3 = 10\sqrt{2}, \xi_4 = 20\sqrt{2}, \xi_5 = 48\sqrt{2}, \xi_6 = 15$$

Eq. (4.23) yields $\beta = \frac{\log_2 6}{5} \approx 0.517$.

$$\begin{array}{c} \text{---} \\ \text{---} \\ \text{---} \\ \text{---} \\ \text{---} \end{array} = \xi_1 \begin{array}{c} \text{---} \\ \text{---} \\ \text{---} \\ \text{---} \\ \text{---} \end{array} + \xi_2 \begin{array}{c} \text{---} \\ \text{---} \\ \text{---} \\ \text{---} \\ \text{---} \end{array} + \xi_3 \begin{array}{c} \text{---} \\ \text{---} \\ \text{---} \\ \text{---} \\ \text{---} \end{array} \quad (4.24)$$

$$+ \xi_4 \begin{array}{c} \text{---} \\ \text{---} \\ \text{---} \\ \text{---} \\ \text{---} \end{array} + \xi_5 \begin{array}{c} \text{---} \\ \text{---} \\ \text{---} \\ \text{---} \\ \text{---} \end{array} + \xi_6 \begin{array}{c} \text{---} \\ \text{---} \\ \text{---} \\ \text{---} \\ \text{---} \end{array}$$

$$\begin{aligned} \xi_1 &= -\frac{5i}{4\sqrt{2}}, \xi_2 = 56 + 8i, \xi_3 = -5, \xi_4 = -(64 + 32i), \xi_5 = -(7\sqrt{2} - \sqrt{2}i), \\ \xi_6 &= -(16 - 48i) \end{aligned}$$

Eq. (4.24) yields $\beta = \frac{\log_2 6}{5} \approx 0.517$.

$$\begin{array}{c} \text{---} \\ \text{---} \\ \text{---} \\ \text{---} \\ \text{---} \end{array} = \xi_1 \begin{array}{c} \text{---} \\ \text{---} \\ \text{---} \\ \text{---} \\ \text{---} \end{array} + \xi_2 \begin{array}{c} \text{---} \\ \text{---} \\ \text{---} \\ \text{---} \\ \text{---} \end{array} + \xi_3 \begin{array}{c} \text{---} \\ \text{---} \\ \text{---} \\ \text{---} \\ \text{---} \end{array} \quad (4.25)$$

$$+ \xi_4 \begin{array}{c} \text{---} \\ \text{---} \\ \text{---} \\ \text{---} \\ \text{---} \end{array} + \xi_5 \begin{array}{c} \text{---} \\ \text{---} \\ \text{---} \\ \text{---} \\ \text{---} \end{array} + \xi_6 \begin{array}{c} \text{---} \\ \text{---} \\ \text{---} \\ \text{---} \\ \text{---} \end{array}$$

$$\begin{aligned} \xi_1 &= \frac{5i}{4\sqrt{2}}, \xi_2 = 56 - 8i, \xi_3 = -5, \xi_4 = -(64 - 32i), \xi_5 = -(\sqrt{2} + 3\sqrt{2}i), \\ \xi_6 &= -(16 + 48i) \end{aligned}$$

Eq. (4.25) yields $\beta = \frac{\log_2 6}{5} \approx 0.517$.

$$\begin{array}{c} \text{---} \\ \text{---} \\ \text{---} \\ \text{---} \\ \text{---} \end{array} = \xi_1 \begin{array}{c} \text{---} \\ \text{---} \\ \text{---} \\ \text{---} \\ \text{---} \end{array} + \xi_2 \begin{array}{c} \text{---} \\ \text{---} \\ \text{---} \\ \text{---} \\ \text{---} \end{array} + \xi_3 \begin{array}{c} \text{---} \\ \text{---} \\ \text{---} \\ \text{---} \\ \text{---} \end{array} \quad (4.26)$$

$$+ \xi_4 \begin{array}{c} \text{---} \\ \text{---} \\ \text{---} \\ \text{---} \\ \text{---} \end{array} + \xi_5 \begin{array}{c} \text{---} \\ \text{---} \\ \text{---} \\ \text{---} \\ \text{---} \end{array}$$

$$\xi_1 = -6 + 2i, \xi_2 = -\frac{5 + 5i}{2}, \xi_3 = -(3\sqrt{2} - \sqrt{2}i), \xi_4 = -(6 - 18i), \xi_5 = \frac{7 + 9i}{2}$$

Eq. (4.26) yields $\beta = \frac{\log_2 5}{4} \approx 0.580$.

$$\begin{array}{c} \text{---} \\ \text{---} \\ \text{---} \\ \text{---} \\ \text{---} \end{array} = \xi_1 \begin{array}{c} \text{---} \\ \text{---} \\ \text{---} \\ \text{---} \\ \text{---} \end{array} + \xi_2 \begin{array}{c} \text{---} \\ \text{---} \\ \text{---} \\ \text{---} \\ \text{---} \end{array} + \xi_3 \begin{array}{c} \text{---} \\ \text{---} \\ \text{---} \\ \text{---} \\ \text{---} \end{array} \quad (4.27)$$

$$+ \xi_4 \begin{array}{c} \text{---} \\ \text{---} \\ \text{---} \\ \text{---} \\ \text{---} \end{array} + \xi_5 \begin{array}{c} \text{---} \\ \text{---} \\ \text{---} \\ \text{---} \\ \text{---} \end{array}$$

$$\xi_1 = -6 + 18i, \xi_2 = -\frac{5 + 5i}{2}, \xi_3 = -(3\sqrt{2} + 11\sqrt{2}i), \xi_4 = -(6 - 2i), \xi_5 = -\frac{1 + 3i}{2}$$

Eq. (4.27) yields $\beta = \frac{\log_2 5}{4} \approx 0.580$.

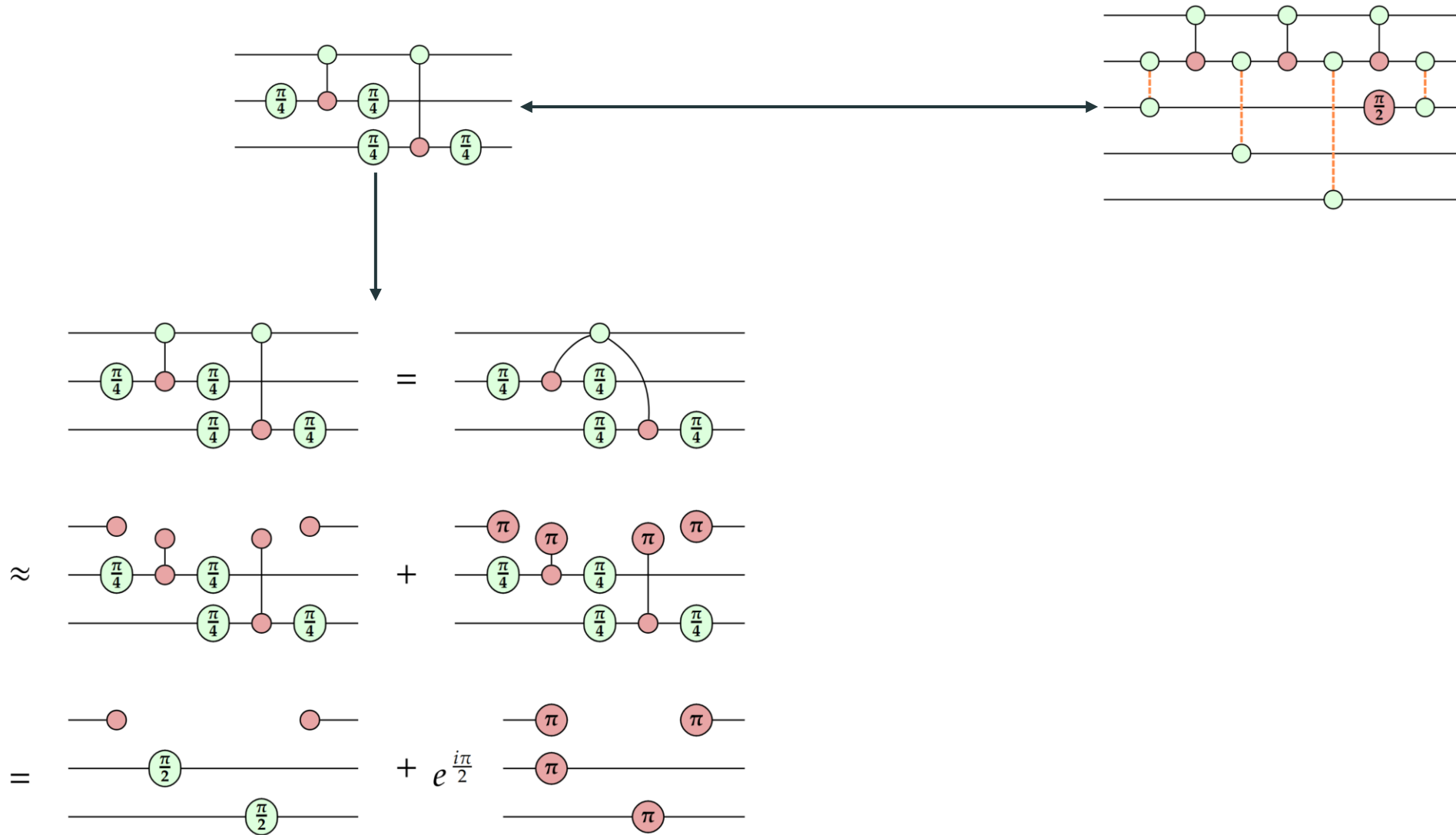
4. Applications

Dynamic decompositions

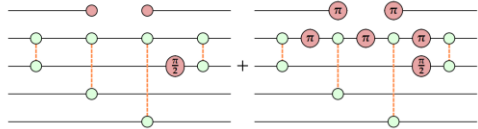
Theorem 5.1.1

$$m \left\{ \begin{array}{c} \vdots \\ \alpha \\ \vdots \end{array} \right\} n = \frac{1}{\sqrt{2}^{n+m}} m \left\{ \begin{array}{cc} \text{---} & \text{---} \\ \vdots & \vdots \\ \text{---} & \text{---} \end{array} \right\} n + \frac{e^{i\alpha}}{\sqrt{2}^{n+m}} m \left\{ \begin{array}{cc} \text{---} & \text{---} \\ \vdots & \vdots \\ \pi & \pi \end{array} \right\} n \quad (5.1)$$

CNOT-grouping



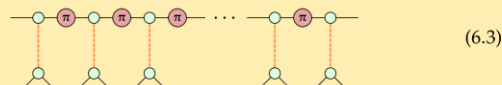
CNOT-grouping



The left term can be simplified by fusing the four Z-spiders. According to Theorem 5.1.3, we can decompose the resulting node, which gives us two terms.

The right term is a bit more difficult due to the new obstructions caused by NOT gates. However, it can be shown that the right term can also be decomposed into two terms, according to Lemma 6.1.1. Therefore, Eq. (6.1) can be decomposed into four terms. But, what would be the final number of terms if a traditional method was used? At first, it might seem that Eq. (4.14) is the best choice. Applying it twice, one obtains nine terms. While this may be true in theory, algorithms that greedily choose the decomposition with the smallest scaling factor will always simplify the diagram after having applied one decomposition. This is exemplified after the following lemma and proof.

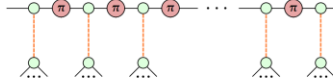
Lemma 6.1.1 Any (sub-)diagram of the form



with m star edges can be rewritten as

$$\left\{ \begin{array}{l} \text{---} \\ \text{---} \\ + \quad \text{---} \\ \text{---} \\ + \quad \text{---} \end{array} \right. \begin{array}{l} \text{if } m \text{ is odd} \\ \text{if } m \text{ is even.} \end{array} \quad (6.4)$$

Proof. The diagram



with m star edges, can be rewritten by using Eq. (4.10), giving us

$$\left\{ \begin{array}{l} \text{---} \\ \text{---} \\ + \quad \text{---} \\ \text{---} \\ + \quad \text{---} \end{array} \right. \begin{array}{l} \text{if } m \text{ is odd} \\ \text{if } m \text{ is even} \end{array} \quad (6.5)$$

$$= \left\{ \begin{array}{l} \text{---} \\ \text{---} \\ + \quad \text{---} \\ \text{---} \\ + \quad \text{---} \end{array} \right. \begin{array}{l} \text{if } m \text{ is odd} \\ \text{if } m \text{ is even.} \end{array} \quad (6.6)$$

The star edges will always be connected to one of the two Z-spiders. We will sometimes refer to these two sides as *stacks*. By decomposing both stacks using Theorem 5.1.3, one obtains four terms, two of which cancel out as they will include an isolated X-spider with a phase of π , which is equivalent to a zero scalar. The final two terms (for both m being odd and even) are given by

$$\begin{aligned} & \text{---} \\ & + \quad \text{---} \\ & + \quad \text{---} \\ & + \quad \text{---} \end{aligned} \quad \begin{array}{l} \text{if } m \text{ is odd} \end{array} \quad (6.7)$$

and

$$\begin{aligned} & \text{---} \\ & + \quad \text{---} \\ & + \quad \text{---} \\ & + \quad \text{---} \end{aligned} \quad \begin{array}{l} \text{if } m \text{ is even} \end{array} \quad (6.8)$$

which can be brought into the desired form of Lemma 6.1.1. \square

Getting back to the reason why such CNOT blockades cannot be exploited like in the T-gate case, let us decompose the first star edge in Eq. (6.2) using Eq. (4.13):

Here, the left term can be further simplified to the following:

$$\begin{aligned} & \text{---} \\ & = \text{---} \\ & \text{(ho), (sp)} \quad = \text{---} \\ & = \sqrt{2} \quad \text{---} \end{aligned}$$

Weighting algorithms

Theorem 5.1.1

$$m \left\{ \begin{array}{c} \text{X-spider} \\ \vdots \end{array} \right\} n = \frac{1}{\sqrt{2}^{n+m}} m \left\{ \begin{array}{c} \text{Z-spider} \\ \vdots \end{array} \right\} n + \frac{e^{i\alpha}}{\sqrt{2}^{n+m}} m \left\{ \begin{array}{c} \text{Z-spider} \\ \vdots \\ \pi \\ \pi \end{array} \right\} n \quad (5.1)$$

```

1 def get_master_v_weight(self, g, v):
2     extra_weight = 2
3     total_weight = 0
4     for l1_nv in g.neighbors(v):
5         if g.phase(l1_nv) != star_phase:
6             continue
7         total_weight += 1
8         l2_nv = list(g.neighbors(l1_nv))
9         l2_nv.remove(v)
10        if len(l2_nv) > 1:
11            continue
12        l2_nv = l2_nv[0]
13        if g.type(l2_nv) != Z:
14            continue
15        l3_nv = list(g.neighbors(l2_nv))
16        l3_nv.remove(l1_nv)
17        for cur_v in l3_nv:
18            if g.phase(cur_v) == star_phase:
19                total_weight += 1
20            elif not g.type(cur_v) in [Z,X]:
21                continue
22            elif g.vertex_degree(cur_v) > 2:
23                continue
24            else:
25                extra_weight_valid = False
26                if g.type(cur_v) == X and g.phase(cur_v) == 1:
27                    extra_weight_valid = True
28                cur_v = list(g.neighbors(cur_v))
29                cur_v.remove(l2_nv)
30                if len(cur_v) > 1:
31                    continue
32                cur_v = cur_v[0]
33                if g.phase(cur_v) != star_phase:
34                    continue
35                total_weight += (extra_weight if extra_weight_valid
36                                else 1)
37
return total_weight

```

The potential master node v has a branch we want to check¹¹:



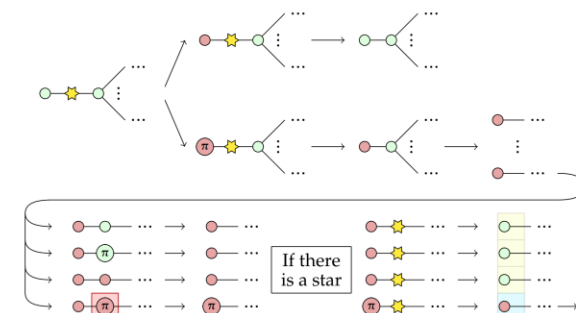
We will only continue searching if the immediate neighbor is a star, in which case the weight is increased by one.



The searching will only continue if there is a Z-spider as its only neighbor, that can potentially have multiple neighbors. It only considers Z-spiders as other patterns were not observed sufficiently enough.

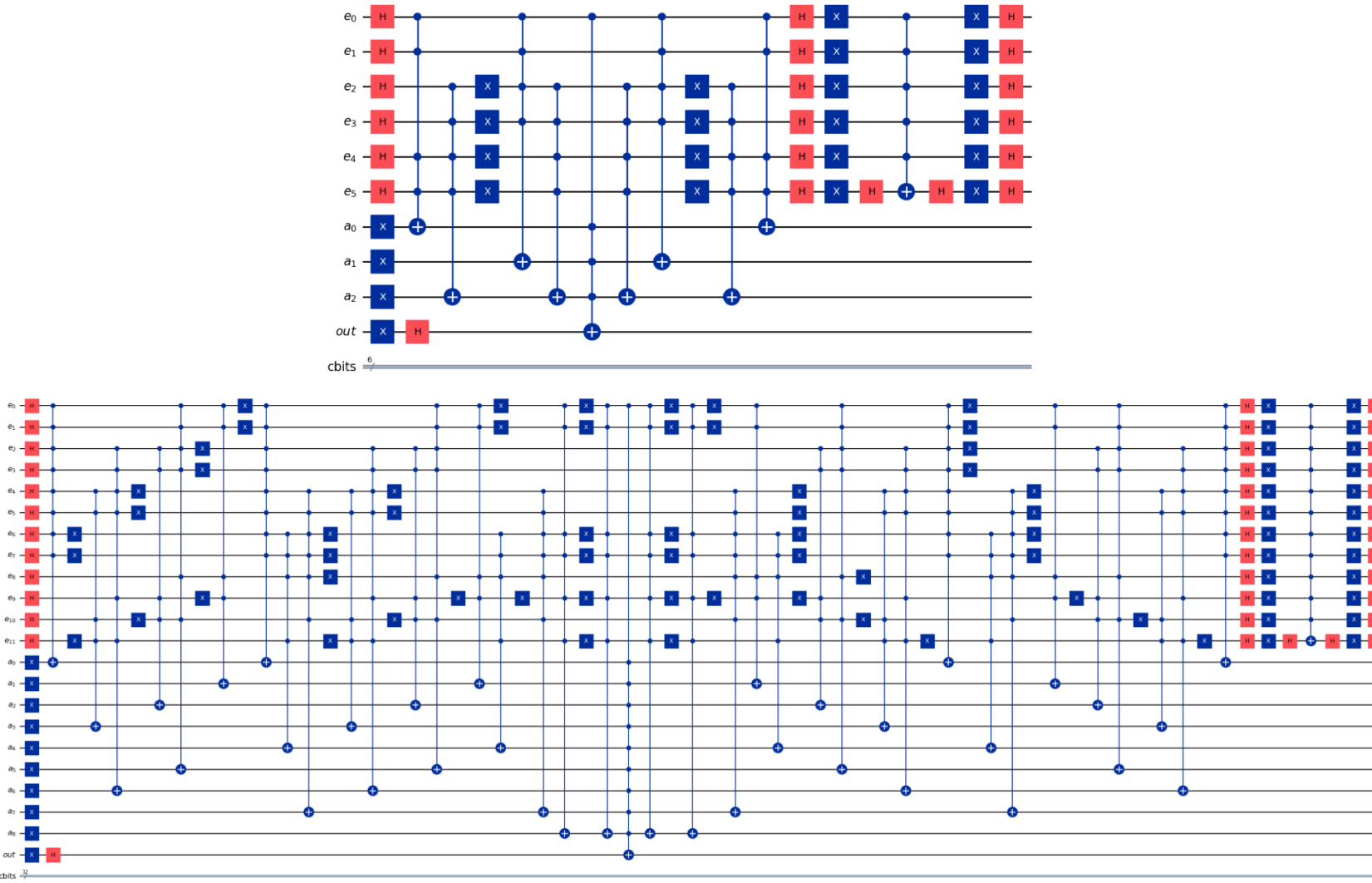


Here, each neighbor is checked. The weight is increased by one if it is a star. Only if the neighbor has a degree of two, the search on that branch is not terminated. If it is an X-spider with phase 0, a Z-spider with phase 0 or π followed by a star, the weight is increased by one. If it is an X-spider with phase π , then the weight is increased by $extra_weight$, which was chosen to be two. The reason for this can be seen in the following illustration, where v is decomposed using Theorem 5.1.1:



In the end, it is clear why an extra weight is useful: An X-spider could remove stars that might follow, whereas a Z-spider could not.

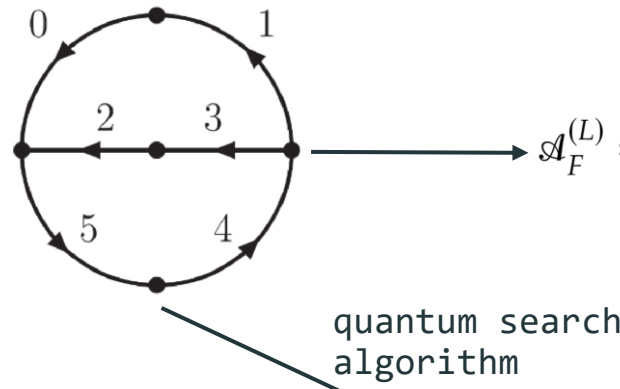
Multi-control Toffoli gate dense quantum circuits



Quantum search algorithm for causal singular configurations of multiloop Feynman diagrams

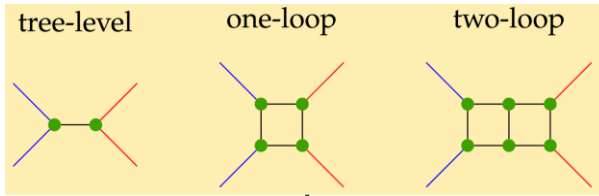
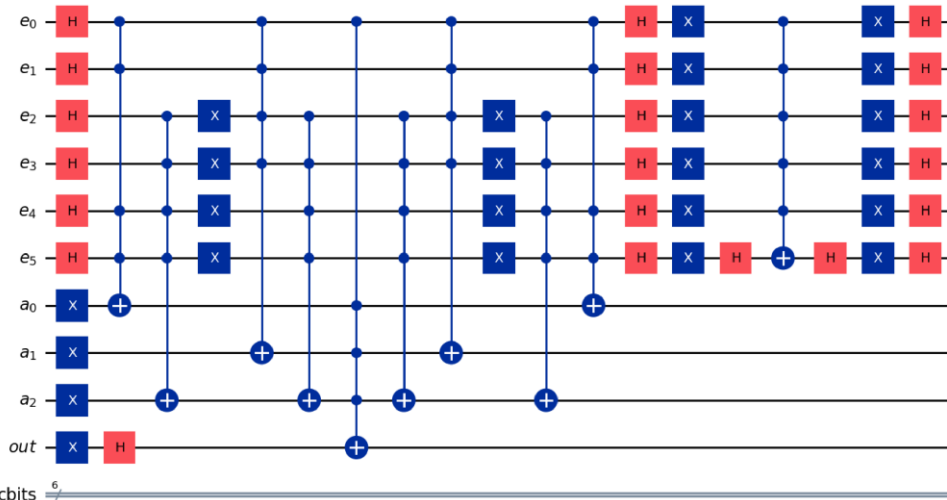
Loop-tree duality formalism

multiloop Feynman diagram



$$= \int_{\ell_1 \dots \ell_L}.$$

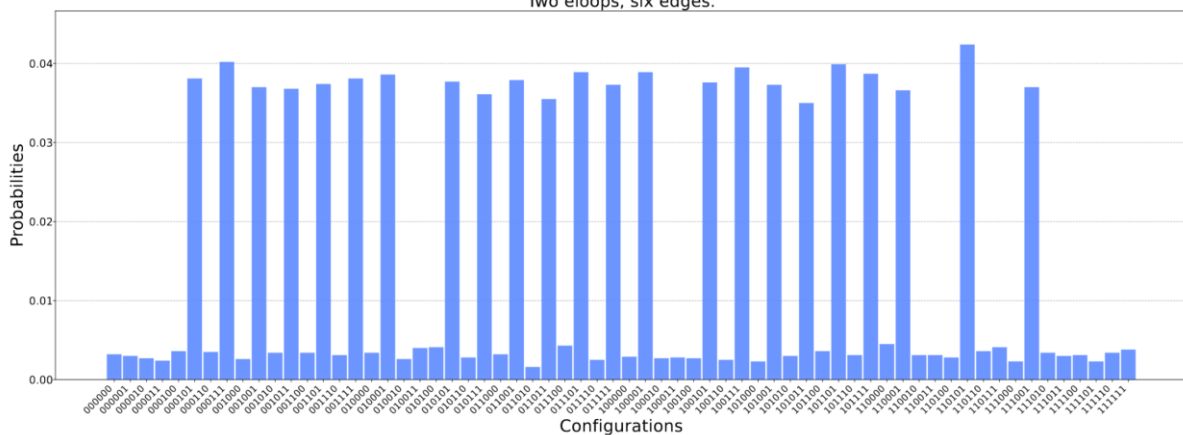
quantum search algorithm



$$\prod_{i=1}^n G_F(q_i) \xrightarrow{\quad \downarrow \quad} \mathcal{A}_D^{(L)} = \int_{\vec{\ell}_1 \dots \vec{\ell}_L} \frac{1}{x_n} \sum_{\sigma \in \Sigma} \frac{\mathcal{N}_{\sigma(i_1, \dots, i_{n-L})}}{h_{\sigma(i_1)} \lambda_{\sigma(i_1)} \dots h_{\sigma(i_{n-L})} \lambda_{\sigma(i_{n-L})}}$$

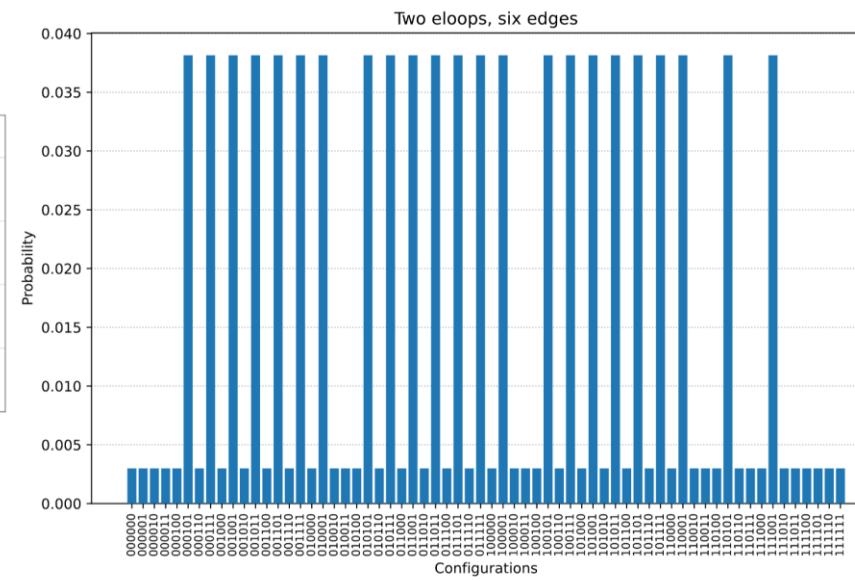
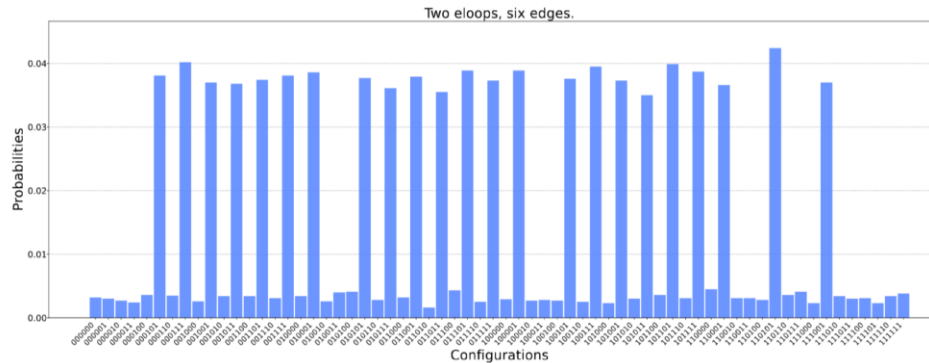
causal singular configurations

Two eloops, six edges



Proof-of-Concept

- Successful simulation:



- Semi-successful decomposition:

	Modified quizx	Our implementation
Two eloop topology	52 terms	48 terms
Four eloop topology	1810 terms	1948 terms

Reason: Partial simplification strategy

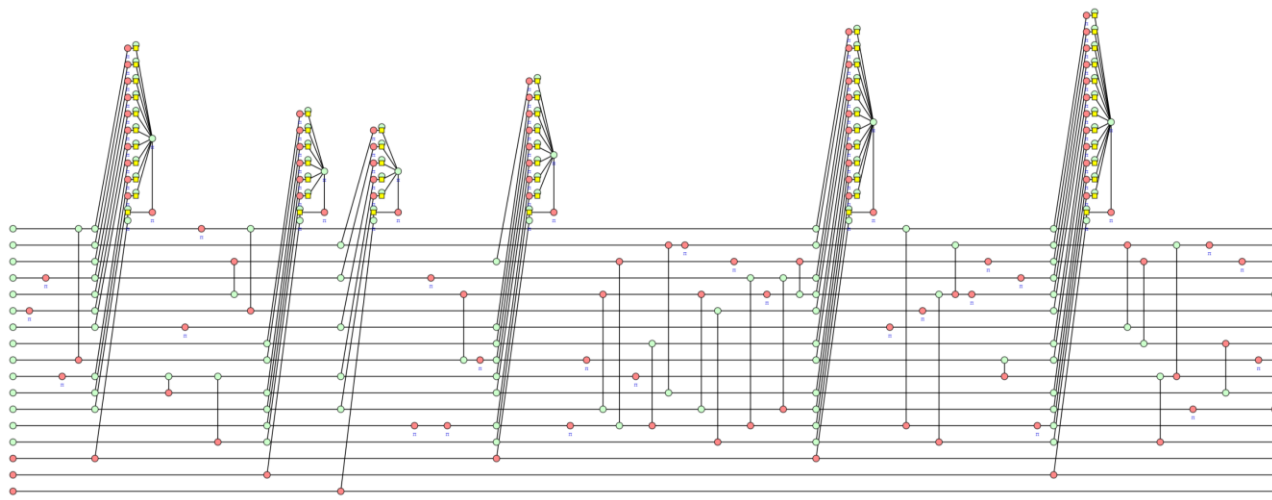


Figure 6.9: The initial 17-qubit scalar diagram before applying any simplification strategy, generated in [101].

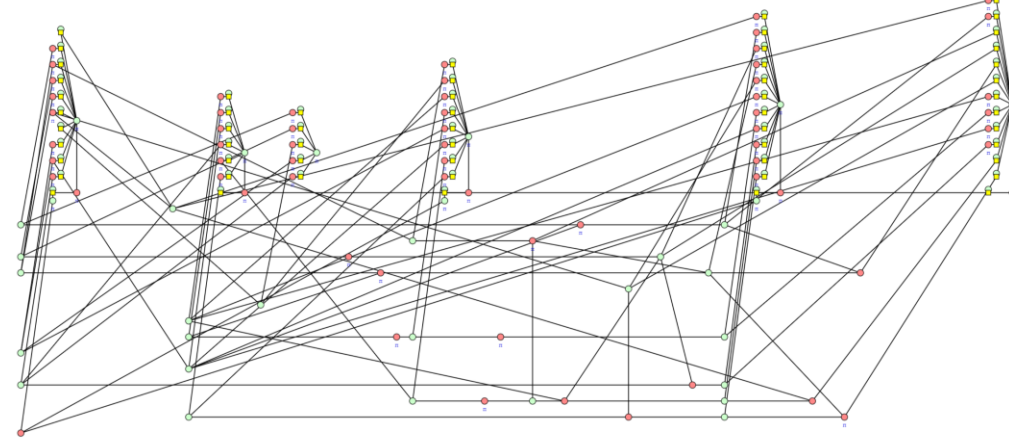


Figure 6.10: The 17-qubit scalar diagram after applying our partial simplification strategy, generated in [101].

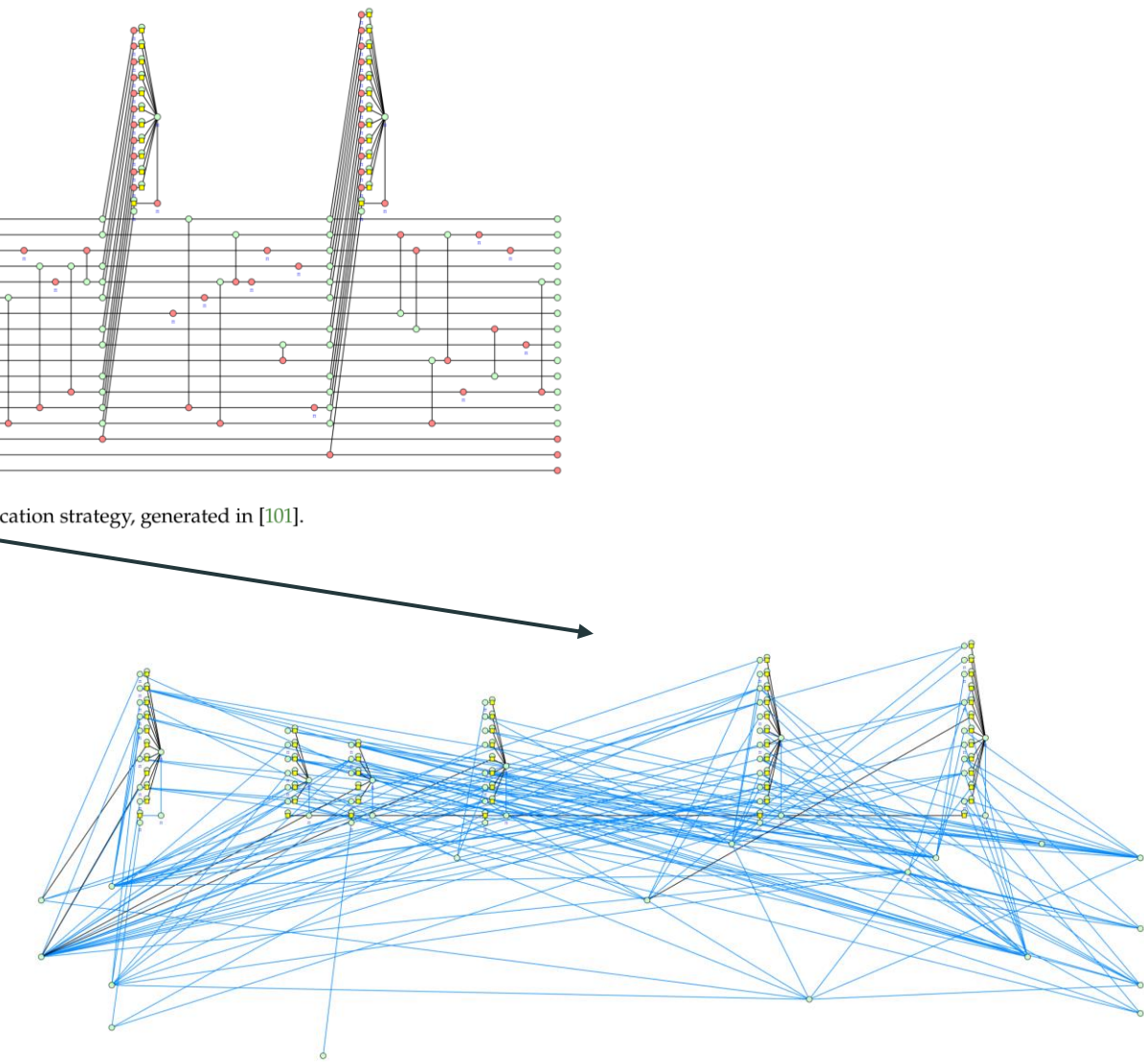
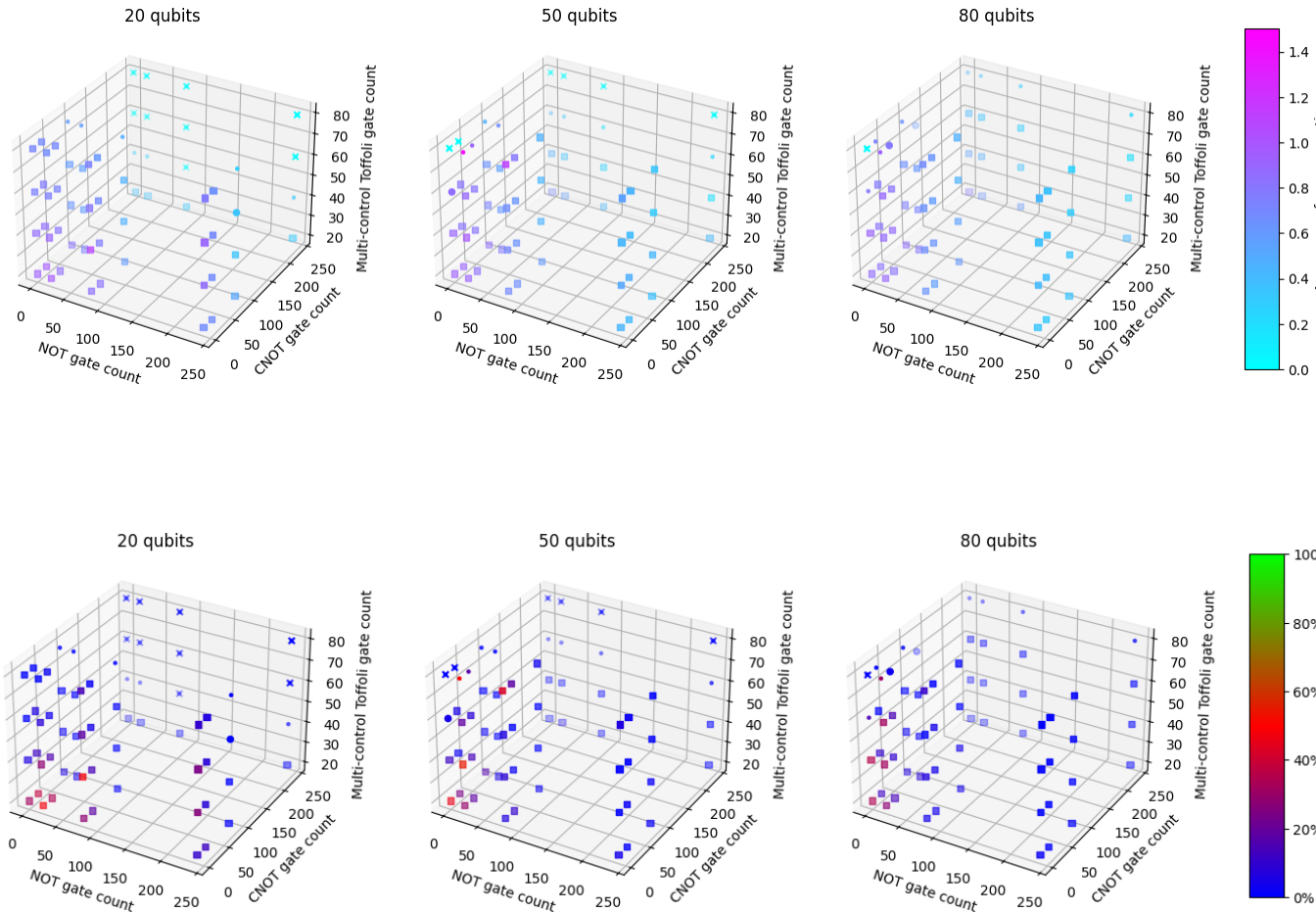


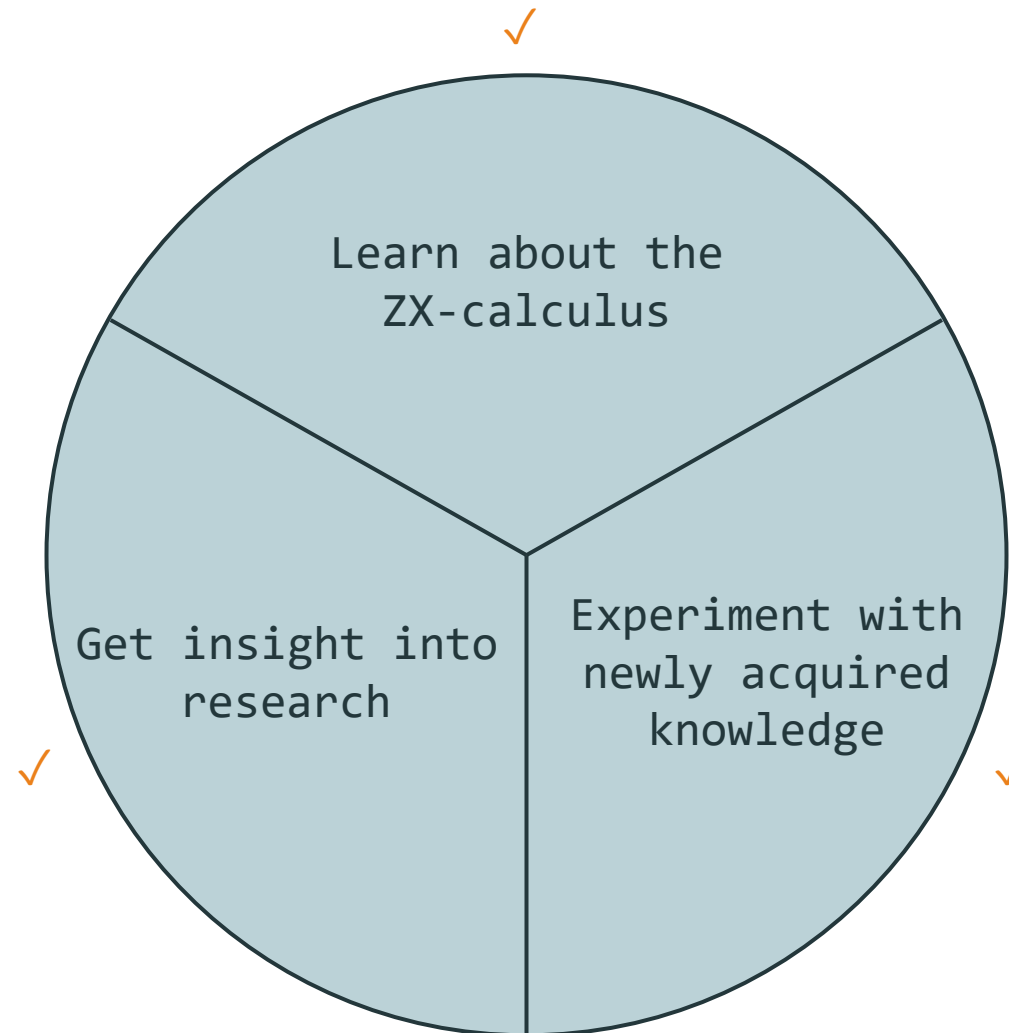
Figure 6.11: The 17-qubit scalar diagram after applying the full simplification strategy, generated in [101].

Reason: Partial simplification strategy



5. Summary

Summary



- Undocumented work
- Novel decompositions (+ HP-computing test)
- Proof for CNOT-grouping using stars
- Simulation of multiloop Feynman diagrams
- Study of weighting algorithms using stars
- (BONUS: Unexpected general improvement)

Acknowledgments

- Thanks to:
 - Dr. Riccardo Ferrario for his supervision
 - the ZX-community for interesting discussions

Thank you for listening!

References

- [1] <https://arxiv.org/list/quant-ph/2025-01>
- [2] <https://quantum-journal.org/>
- [3] <https://zxcalculus.com/publications.html>
- [4] <https://indico.cern.ch/event/421552/sessions/170249/attachments/884224/1242865/feynman.pdf>
- [5] https://www.researchgate.net/figure/Detection-logic-circuits-using-an-AND-gate-to-assert-the-control-signal_fig3_3338000
- [6] <http://homepages.math.uic.edu/~kauffman/Penrose.pdf>
- [7] <https://en.wikipedia.org/wiki/ZX-calculus>
- [8] <https://vdwetering.name/pdfs/presentation-zx-compilation.pdf>
- [9] [https://en.wikipedia.org/wiki/Simulated annealing#/media/File:Hill Climbing with Simulated Annealing.gif](https://en.wikipedia.org/wiki/Simulated_annealing#/media/File:Hill_Climbing_with_Simulated_Annealing.gif)

Questions?

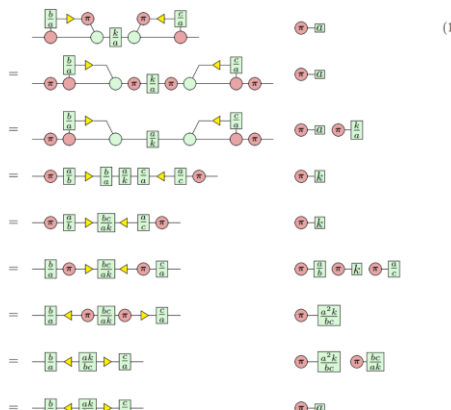
Appendix

Appendix: Undocumented work (2 examples)

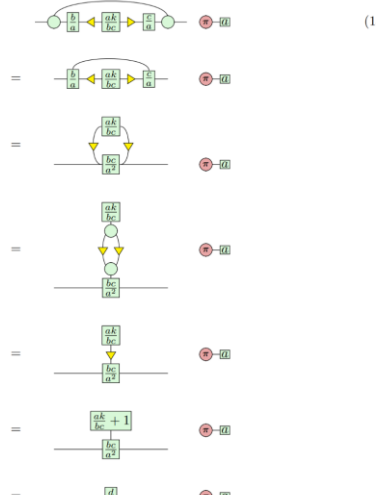
- Validity proof of quantum query algorithm:

$$\mathbb{E}_\theta(f) = \left(\frac{1}{2\pi}\right)^n \int_{[0,2\pi]^n} f(\theta) d\theta$$

First, we will simplify M_σ as in Lemma 4:



for which we can use Lemma 3, so:



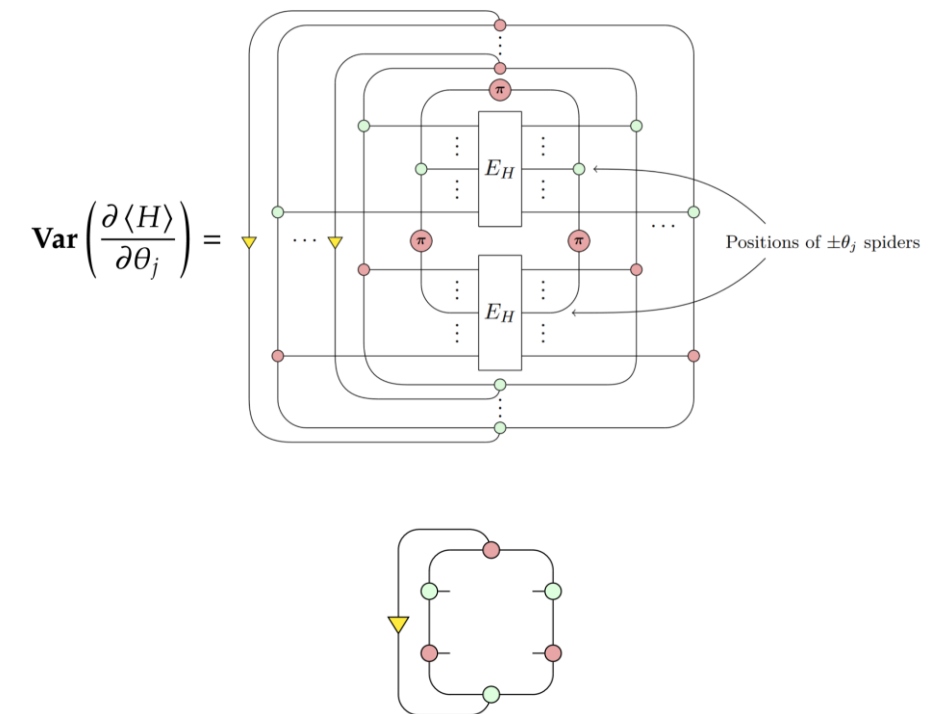
Now using Lemma 5 we obtain:



Finally, we can evaluate the definite integral:

$$\begin{aligned} \phi(\sigma) &= \frac{1}{2\pi} \int_{-\pi}^{\pi} R_\theta^\dagger M_\sigma R_\theta d\theta \\ &= \frac{1}{2\pi} \int_{-\pi}^{\pi} \left(\begin{array}{c} 0 \\ \text{CNOT}(b,c) \\ \text{R}_b(\theta) \\ \text{CNOT}(a,c) \\ \text{R}_a(\theta) \end{array} \right) \left(\begin{array}{c} 0 \\ \text{CNOT}(b,c) \\ \text{R}_b(-\theta) \\ \text{CNOT}(a,c) \\ \text{R}_a(-\theta) \end{array} \right) d\theta \end{aligned} \quad (14)$$

- Decomposition of cycles



$$\text{Var}\left(\frac{\partial \langle H \rangle}{\partial \theta_j}\right) =$$

Which in matrix notation is the following:

$$\begin{pmatrix} 1 & 0 \\ 0 & d \end{pmatrix} \cdot a = \begin{pmatrix} a & 0 \\ 0 & d \end{pmatrix} \quad (16)$$

This completes the proof for $n = 1$.

To inductively provide a proof for $n > 1$, consider the explicit form of $\phi(\sigma)$ by substituting Equation (4) into it:

$$\begin{aligned} \phi(\sigma) &= \left(\frac{1}{2\pi} \int_0^{2\pi} d\theta_1 \right) \circ \dots \circ \left(\frac{1}{2\pi} \int_0^{2\pi} d\theta_n \right) f(\theta_1, \theta_2, \dots, \theta_n) \\ &= \left(\frac{1}{2\pi} \int_0^{2\pi} d\theta_1 \right) \circ \dots \circ \left(\frac{1}{2\pi} \int_0^{2\pi} d\theta_n \right) (R_{\theta_1}^\dagger M_1 R_{\theta_1} \otimes \dots \otimes R_{\theta_n}^\dagger M_n R_{\theta_n}) \end{aligned} \quad (17)$$

Since the operator $\frac{1}{2\pi} \int_0^{2\pi} d\theta_i$ leaves any constants unchanged, it effectively only changes the term $R_{\theta_i}^\dagger M_i R_{\theta_i}$ in the tensor product. This change is what we proved for the $n = 1$ case, i.e. it sends M_σ to its diagonal entries (we denote the matrix only consisting of the diagonal

Appendix: Unexpected improvement

Theorem 5.1.1

$$m \left\{ \begin{array}{c} \vdots \\ \alpha \\ \vdots \end{array} \right\} n = \frac{1}{\sqrt{2}^{n+m}} m \left\{ \begin{array}{c} \vdots \\ \text{pink} \\ \vdots \end{array} \right\} n + \frac{e^{i\alpha}}{\sqrt{2}^{n+m}} m \left\{ \begin{array}{c} \vdots \\ \text{purple} \\ \vdots \end{array} \right\} n \quad (5.1)$$

$$= \sqrt{2} \left(\text{diagram with } \pi \text{ on top} \right) + 2 \left(\text{diagram with } \pi \text{ on bottom} \right) \quad (4.13)$$

$$= \frac{1}{\sqrt{2}} \left(\text{diagram with } \pi \text{ on top} \right) + \frac{1}{\sqrt{2}} \left(\text{diagram with } \pi \text{ on bottom} \right) + 4 \left(\text{diagram with } 2 \pi \text{ on top} \right) \quad (4.14)$$

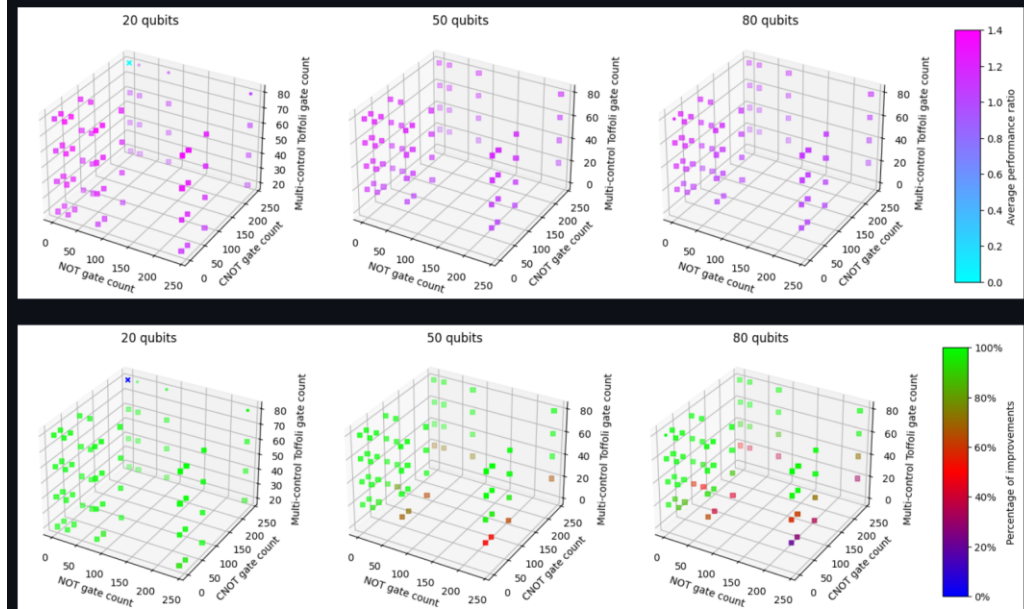
$$\begin{aligned} &= \frac{1}{2\sqrt{2}} \left(\text{diagram with } \pi \text{ on top} \right) + \frac{1}{2\sqrt{2}} \left(\text{diagram with } \pi \text{ on bottom} \right) + \frac{1}{2\sqrt{2}} \left(\text{diagram with } 2 \pi \text{ on top} \right) \\ &\quad + \frac{1}{\sqrt{2}} \left(\text{diagram with } 3 \pi \text{ on top} \right) + 8 \left(\text{diagram with } 4 \pi \text{ on top} \right) \quad (4.15) \end{aligned}$$

unexpected_improv_of_speedy_algo

This unfinished investigation found that utilizing star decompositions in the greedy algorithm proposed in "[Speedy Contraction of ZX Diagrams with Triangles via Stabiliser Decompositions](#)" is only beneficial in certain cases, and might hurt the performance in others (where instead dynamic decompositions are used).

In particular, this [log file](#) seems to suggest that the use is justified for the application to quantum machine learning ansätze, as on average it performs much better than the version that does not use star decompositions (in certain cases it is slightly worse, but in most cases it is either as good or significantly better).

On the other hand, when using the version without star decompositions for the tested randomly generated multi-control Toffoli gate dense quantum circuits, we can observe reliable improvements over the original implementation:



Although the exact reasons for this behavior would need to be investigated, one possible explanation could be the following. When using star decompositions, the resulting terms contain newly added states, consisting of X-spiders, and more importantly, Z-spiders. In contrast, dynamic decompositions only contain X-spiders. They have the pleasant property of being able to turn neighboring star edges into Clifford states, which turns out to be a common pattern. Although technically possible (in case the star edge is not an immediate neighbor), this occurs a lot less for Z-spiders. A potential reason for why this could positively affect multi-control Toffoli gates is that those circuits tend to be highly-interconnected. Therefore, potential simplifications resulting from X-spiders could outweigh a slight advantage of star decompositions with regard to their scaling. Conversely, this might not be the case for the less interconnected quantum machine learning diagrams.